

# Polypyrrole doped zirconium dioxide composite as electrode material for super-capacitor applications

F Zhao<sup>1</sup>, M Irfan<sup>2\*</sup>, W Abbas<sup>2\*</sup>, G F B Solre<sup>3</sup>, B A Al-Asbahi<sup>4</sup> and S M H Qaid<sup>4</sup>

<sup>1</sup>Mechanical and Electrical Engineering College, Hainan Vocational University of Science and Technology, Hainan 587000, People's Republic of China

<sup>2</sup>Institute of Physics, Bahauddin Zakriya University, Multan 60800, Pakistan

<sup>3</sup>Department of Chemistry, Thomas J. R. Faulkner College of Science and Technology, University of Liberia, 00231 Monrovia, Montserrado County, Liberia

<sup>4</sup>Department of Physics and Astronomy, College of Science, King Saud University, P.O. Box 2455, 11451 Riyadh, Saudi Arabia

Received: 14 March 2024 / Accepted: 11 July 2024

**Abstract:** A PPy-ZrO<sub>2</sub> composite was synthesized using in-situ polymerization, resulting in polypyrrole-doped Zirconium dioxide. This composite was then studied for its electrochemical characteristics as an electrode material in supercapacitors. The X-ray diffraction (XRD) study confirmed the formation of the composite. Scanning Electron Microscopy (SEM) also confirms platelet structure in the PPy-ZrO<sub>2</sub> composite. Fourier transform infrared (FTIR) analysis showed strong interaction between PPy and ZrO<sub>2</sub> nanoparticles. Synthesized samples are characterized and assessed by impedance, cyclic voltammogram, and galvanostatic charge/discharge. The maximum specific capacitance of 1265 Fg<sup>-1</sup> at 1 Ag<sup>-1</sup> is observed at PPy-ZrO<sub>2</sub> electrodes. The energy density of 28 Wh kg<sup>-1</sup> is found at 378 W kg<sup>-1</sup> (power density), and the impedance of pure PPy ~ 13 Ω to PPy-ZrO<sub>2</sub> ~ 11 Ω of the composite is decreased, which may represent a beneficial effect of ZrO<sub>2</sub>-particles and PPy for the development of an electrode material.

**Keywords:** Metal oxide; Conducting polymer; Electrode material; Energy storage; Supercapacitor

## 1. Introduction

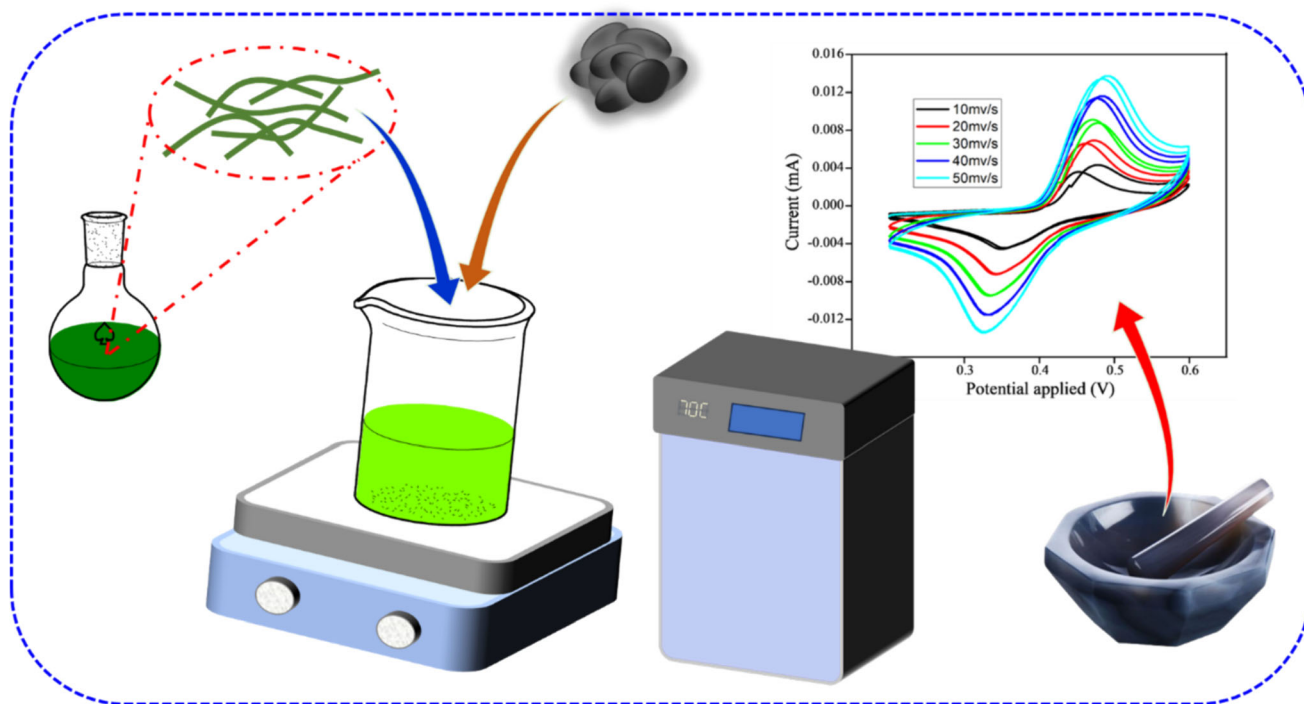
Nanocrystalline metal oxide, P-type semiconductors have been broadly focused through investigators in recent decades due to their wide applications [1–6]. Zirconium dioxide (ZrO<sub>2</sub>) is a wide band gap of 5.3 eV P-type semiconductor and shows rich oxygen vacancies on its surface [7–10]. ZrO<sub>2</sub> is a material of excessive technological significance, having durability, chemical stability, a natural white color, and splendid rust resistance [11–15]. The ZrO<sub>2</sub> has potential applications in piezoelectric and semiconductor devices such as photodiodes, transparent electrodes, solar cells, catalysts, and gas sensors [16–21]. On the other hand, the conducting polymers have an extensive series of applications, for instance, sensors that sense the vapor of different gases, Schottky diodes, field-

effect transistors, and light-emitting diodes [22–26]. The PPy is known as a positive conducting polymer widely used to synthesize composites owing to its simple synthesis, good compatibility, high electrical conductivity, and excellent ecological stability [27–30]. Its chemical formula is C<sub>4</sub>H<sub>4</sub>NH, and the chemical structure of polypyrrole is exhibited in Scheme 1. The electrical conductivity of polypyrrole can be improved by incorporating inorganic fillers; furthermore, the conductivity of polypyrrole depends on dopant ions [31–35]. Quite a few researchers have more attention to investigating the conducting polymer/inorganic-particle composites that might show outstanding physical and mechanical characteristics [36, 37]. Niaz et al. reported the synthesis of MoS<sub>2</sub>-polypyrrole nanocomposites using a hydrothermal method, serving as supercapacitor electrodes. The layered structure aids proton movement, enhancing accessibility and shortening ion path length. Stable electrodes with 95% capacitance retention after 500 cycles are achieved, outperforming pure polypyrrole [38]. Another report synthesized a quaternary

\*Corresponding author, E-mail: mirfanphysics@gmail.com; Dr.waseemabbas@bzu.edu.pk

PANI-Pr<sub>2</sub>O<sub>3</sub>-NiO-Co<sub>3</sub>O<sub>4</sub> core-shell nanocomposite using coprecipitation and ultra-sonication methods. The study concludes that this nanocomposite offers higher capacitance, aiding ion transfer and core-shell structure formation to enhance surface-related electrochemical properties [39]. Boutaleb et al. synthesized PANI-TiO<sub>2</sub>-CuO ternary composite by using the in-situ oxidative polymerization route. They reported that the as-synthesized composite was good at holding its capacity, keeping 87.5% of its energy storage ability after 1500 cycles [40]. Zenasni et al. explored the ZrO<sub>2</sub>-ZnO doped polypyrrole composites as an electrode material that was synthesized using an in-situ polymerization technique. The electrochemical properties of electrode materials are confirmed by cyclic voltammetry, galvanostatic charge and discharge, and electrochemical impedance spectroscopy. Additionally, the electrode stability was also determined which showed specific capacitance retention of 90.2% for synthesized composites after cycling up to 4000 cycles. The synthesized PPy-ZrO<sub>2</sub>-ZnO composites act as an organic semiconductor material and can be developed as the electrode material. Numerous investigators have studied that the development of efficient charge packing materials is a key to upcoming renewable energy organization. They were seen that the present research work might be a maximum auspicious alternative to constant storage of electrical energy in a supercapacitor electrode [41]. Ullah et al. investigated the polypyrrole

(PPy), which doped a higher weight percentage of zirconium dioxide nanoparticle composites synthesized via the in-situ chemical oxidative technique. The synthesized composites were analyzed for electrochemical features of the electrode are sightseen by cyclic voltammetry and galvanostatic charge/discharge process. Also, the composite materials maintain stability after 1000 charge and discharge cycles, with 85% capacitance retention at 1 A g<sup>-1</sup>. The synthesized composites may behave as semiconductors and might be developed as an electrode material. Compared to other metallic materials, the synthesized materials can be used to fabricate electrode material and make the procedure eco-friendly. Many researchers observed that the prepared composites were very useful and played an emerging part in the field of material science research in fabricating electrodes for high-performance supercapacitor applications [42]. Similarly, PPy-inorganic-filler composites were synthesized utilizing metal oxides like TiO<sub>2</sub>, Fe<sub>3</sub>O<sub>4</sub>, MnO<sub>2</sub>, Y<sub>2</sub>O<sub>3</sub>, and ZrO<sub>2</sub> have been reported [43–47]. However, current electrode materials face challenges such as poor stability, low energy density, and high self-charge/discharge rates in supercapacitors. Therefore, there is a crucial need to synthesize new electrode materials with enhanced electrochemical properties for the design of the next generation of supercapacitors. In this work, the low weight ratio of ZrO<sub>2</sub> dopant was added into the polypyrrole to synthesize the PPy-ZrO<sub>2</sub> composite via oxidative



**Scheme 1** Schematic illustration of synthesis route and results of PPy-ZrO<sub>2</sub> composite

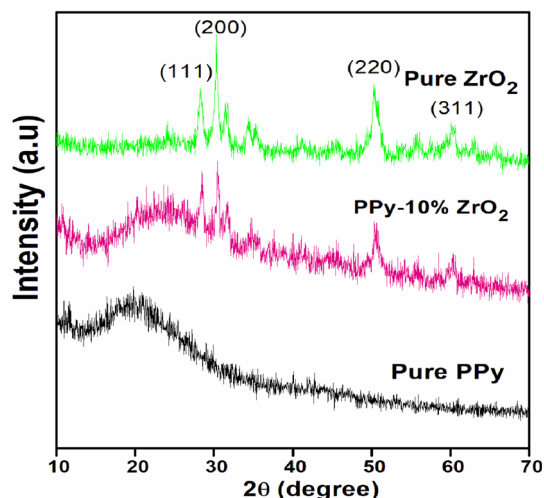


**Fig. 1** XRD profiles for PPy, PPy-ZrO<sub>2</sub> composite, and Pure ZrO<sub>2</sub>

chemical polymerization technique. The structural characterization techniques were utilized to analyze the structure of the PPy-ZrO<sub>2</sub> composite and electrochemical measurements have been applied to study the effect of ZrO<sub>2</sub> on the electrochemical properties of the composite. The resulting PPy-ZrO<sub>2</sub>-designed electrode material displays improved performance in supercapacitor applications.

## 2. Preparation of PPy-ZrO<sub>2</sub> composite

Pyrrrole was bought from Riedel-de-Haen. Duksan Chemicals delivers ammonium persulfate. The Zirconium dioxide (0.25 gm) was bought from UNI-CHcM chemicals, and the Hydrochloric acid was purchased from Sacharlu. All material was utilized conventionally except pyrrole. The chemical polymerization technique synthesizes polypyrrole in an open environment and uses APS as an oxidant (Scheme 1). The molar ratio of monomer to oxidant was kept 1:1. The APS (8.5 g) was dispersed into 100 mL deionized water and strongly stirred for 30 min at 30 °C. After that, 2.5 mL of pyrrole was inserted into 100 mL deionized water, and 5 mL HCl was introduced dropwise to keep the pH between 0 and 1. After 30 min, both solutions

**Table 1** X-ray diffraction data for pristine ZrO<sub>2</sub>

2θ (deg)	d-spacing (nm)	hkl
28.24	0.32	111
30.39	0.29	200
50.44	0.18	220
60.27	0.15	311

were miscellaneous as well and stirred for 3 h. The solution was left overnight in an open environment to get complete polymerization. Lastly, got greenish-black solution was filtered via filter paper and then washed again and again with de-ionizing water to eliminate the HCl from the solution. The suspension was located at 70 °C in a vacuum oven to dehydrate and then ground to fine powder of polypyrrole was obtained. The PPy-ZrO<sub>2</sub> composite was synthesized in the same as the synthesis of polypyrrole has been discussed above.

## 3. Measurements

The X-ray diffraction was carried out utilizing the automated diffractometer, Panalytical X-Pert PRO instrument. The scanning electron microscope was carried out on an EVO50 ZEISS machine. CV was performed to evaluate electrochemical properties at 30 °C with 1-M KOH electrolyte and mass of the sample 0.00025 g. Electrochemical impedance spectroscopy (Impedance Analyzer-PGSTAT-204 (AUT-50296)) measurement was performed from 100 kHz-0.1 Hz frequency range for an open circuit with AC perturbation of 5 mV at 10–50 mV/s scan rates with a potential window from 0.2 to 0.6 V.

## 4. Results and discussion

### 4.1. Structural analysis

Figure 1 exhibits PPy, PPy-ZrO<sub>2</sub> composite XRD profiles and pristine ZrO<sub>2</sub>-nanoparticles. It is clear from the XRD pattern, the pure ZrO<sub>2</sub> was a tetragonal structure with main

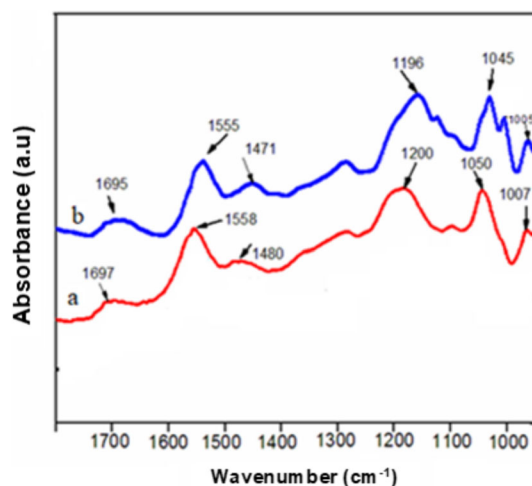


**Fig. 2** FTIR spectra of (a) Pure PPy (b) PPy-10% ZrO<sub>2</sub> composite

peaks observed at  $2\theta = 28.24^\circ$ ,  $30.39^\circ$ ,  $50.44^\circ$ , and  $60.27^\circ$  representing the [111], [200], [220] and [311] planes are in good agreement with that of with JCPDS No. 70-1769 [48]. Scherrer's equation, utilized to calculate the crystallite size of  $ZrO_2$  was found 30.4 nm. The XRD pattern for pure PPy defines the amorphous nature because a broad peak was found in the  $2\theta$  range  $17^\circ$ – $22^\circ$  [49]. Bragg's equation was utilized to compute the experimental d-values [50]. The core crystalline peaks of  $ZrO_2$  at  $2\theta$  values correspond to the periodicity in the direction of [hkl] planes and the degree of crystallinity is summarized in Table 1. The XRD pattern of the PPy- $ZrO_2$  composite shows the characteristic peaks of  $ZrO_2$  present in PPy also presented in Fig. 2. This study confirmed that the composite is composed of  $ZrO_2$ -particles and PPy, and there is an increase in crystallinity [48].

#### 4.2. FTIR analysis

Figure 2 presented the FTIR Spectra of pristine PPy, and PPy-10%  $ZrO_2$  composite, where significant changes were observed more clearly between PPy and PPy- $ZrO_2$  composite. The band observed at  $1045\text{ cm}^{-1}$  corresponds to symmetric C–H in the plane mode. The band at  $1205\text{ cm}^{-1}$  is the N–H in the plane mode and it was the typical band for PPy. The band at  $1560\text{ cm}^{-1}$  and  $1470\text{ cm}^{-1}$  corresponds to C–C and C=C stretching vibrations. The bands observed in the present study are consistent with the reported literature and confirm the formation of polypyrrole [51]. However, the characteristic bands of PPy were shifted from  $1055$  to  $1035\text{ cm}^{-1}$ ,  $1205$  to  $1160\text{ cm}^{-1}$ ,  $1470$  to  $1450\text{ cm}^{-1}$ ,  $1560$  to  $1540\text{ cm}^{-1}$ , and  $1705$  to  $1690\text{ cm}^{-1}$  in the PPy- $ZrO_2$  composite towards the lower wave numbers are plotted in Fig. 2(b). From this study, it

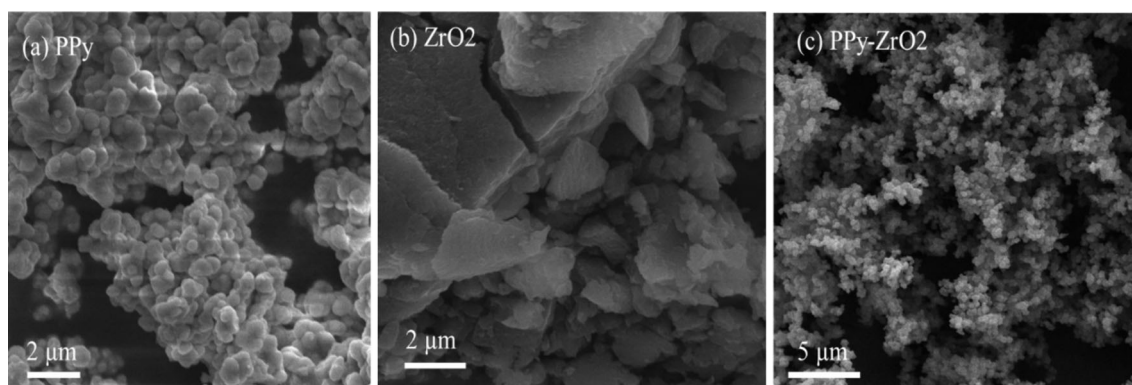


**Fig. 3** SEM micrographs of (a) Pure PPy (b) Pristine  $ZrO_2$  (c) PPy- $ZrO_2$  composite

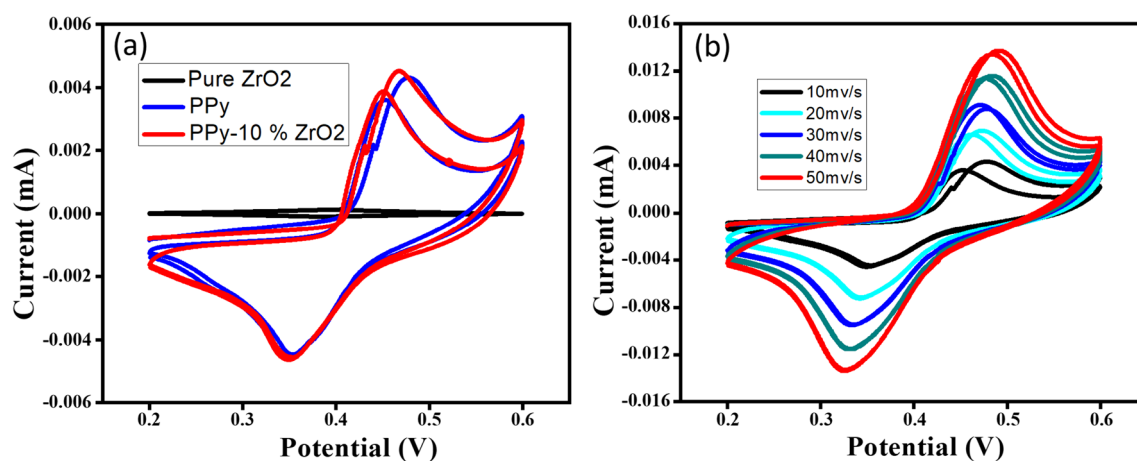


**Fig. 4** (a) CV curves of  $ZrO_2$ , PPy, and PPy- $ZrO_2$  composite at 10 mV/s scan, and (b) CV curves of PPy-10%  $ZrO_2$  composite at different scan rates

**Table 2** Cs (Fg<sup>-1</sup>) of ZrO<sub>2</sub>, PPy, and PPy-10% ZrO<sub>2</sub> composite at scan rate of 10 mV/s

Samples	Specific capacitance (Fg <sup>-1</sup> )
ZrO <sub>2</sub>	27
PPy	279
PPy-10% ZrO <sub>2</sub>	960

**Table 3** Cs (Fg<sup>-1</sup>) of PPy-10% ZrO<sub>2</sub> at different scan rates

10 mV/s	20 mV/s	30 mV/s	40 mV/s	50 mV/s
960 Fg <sup>-1</sup>	880 Fg <sup>-1</sup>	827 Fg <sup>-1</sup>	760 Fg <sup>-1</sup>	736 Fg <sup>-1</sup>

may be concluded that an interaction exists between the interface of PPy and ZrO<sub>2</sub> particles [52].

#### 4.3. Surface morphological analysis

The surface morphology of all samples was explored by SEM analysis. To confirm the increased in crystallinity of polypyrrole and also mixed with ZrO<sub>2</sub>, the morphology of pure ZrO<sub>2</sub> and synthesized PPy-10%ZrO<sub>2</sub> composite were studied and their images are shown in Fig. 3. The SEM images show the hemispherical nature of polymer as clusters in PPy-ZrO<sub>2</sub> composite and platelet structure of pristine ZrO<sub>2</sub>. The ZrO<sub>2</sub>-particles are bound into the PPy chain because of vigorous nanoparticle interaction (Fig. 3(a, b)). SEM and XRD studies show that the PPy-10% ZrO<sub>2</sub> composite is more crystalline than synthesized pristine PPy. This study shows that the PPy-ZrO<sub>2</sub> composite has seen more progress in particle size (2-μm estimated) and an eggshell structure.

**Table 4** Capacitance, energy density, and power density for ZrO<sub>2</sub>, PPy, and its composite at 1A/g

Samples at 1A/g	Capacitance (Fg <sup>-1</sup> )	Energy density (W h Kg <sup>-1</sup> )	Power density (W Kg <sup>-1</sup> )
ZrO <sub>2</sub>	69	2	35
PPy	749	17	286
PPy-10% ZrO <sub>2</sub>	1265	28	378

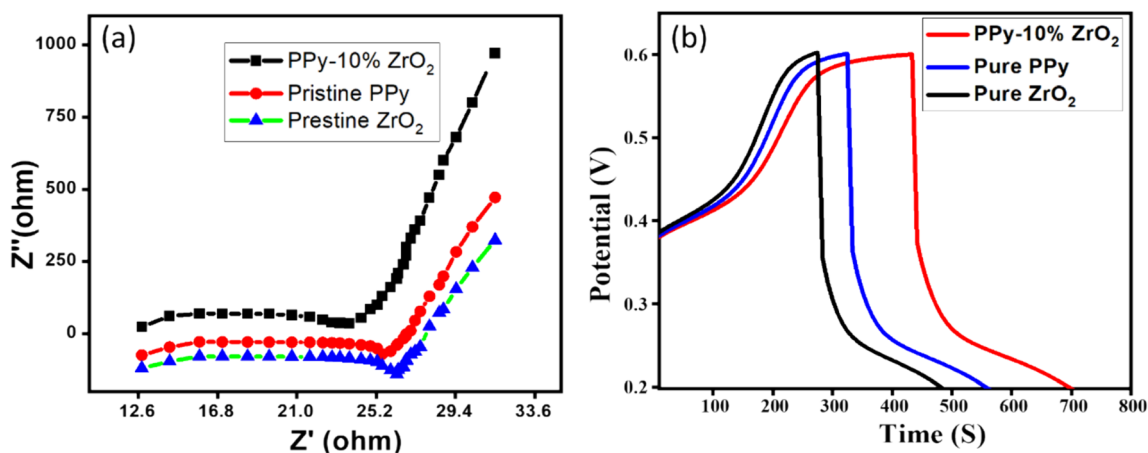
#### 4.4. Supercapacitive analysis

Figure 4(a) shows CV curves for ZrO<sub>2</sub>, PPy, and PPy-10%ZrO<sub>2</sub> composite. Individual redox peaks were detected in PPy, and also in PPy-ZrO<sub>2</sub> nanocomposite electrodes were moved positively and negatively due to the resistance of the electrode; however, the CV of ZrO<sub>2</sub> shows the pseudo-rectangular form except any redox peak was plotted in Fig. 3(a). This classifies ZrO<sub>2</sub> as an individual electrical binary layer super-capacitor.

The specific capacitance of all the samples was calculated and given in Table 2. Cyclic Voltammetry (CV) was executed to investigate the electrochemical properties of polypyrrole (PPy) and PPy-ZrO<sub>2</sub> composite by incorporating 10% ZrO<sub>2</sub>-nanoparticles. Figure 4(b). displays CV curves of PPy-ZrO<sub>2</sub> nanocomposite at 20–50 mV/s scan rates with a potential window from 0.2 to 0.6 V. It is clear from the graphs that the anodic cathodic performance increases positively and negatively with raising the scan rates. The Cs are reduced by enhancing the scan rates. The Cs is measured by using the following relation

$$C_s = I \int dV/m \Delta V \quad (1)$$

In the above Eq. (1), the symbol “I” is current, “dV”


**Fig. 5** (a) Comparison of Nyquist graphs of PPy-ZrO<sub>2</sub>, PPy, and ZrO<sub>2</sub> in 5 mV AC perturbations. (b) Galvanostatic charge/discharge ZrO<sub>2</sub>, PPy, and PPy-ZrO<sub>2</sub> composite at 1 Ag<sup>-1</sup>

**Table 5** Comparative investigation of PPy-ZrO<sub>2</sub> with other electrode materials

S. no.	Electrode material	Specific capacitance (F g <sup>-1</sup> )	Energy density (Wh kg <sup>-1</sup> )	Power density (Wh kg <sup>-1</sup> )	References
1	PANI-RGO-ZnO	40	5.61	403	[56]
2	PPy-GO-ZnO	94.6	10.65	258.26	[57]
3	rGO-MnFe <sub>2</sub> O <sub>4</sub> -PPy	232	32.3	581	[58]
4	MWCNT-PPy-MnO <sub>2</sub>	270	36	500	[59]
5	rGO-CNT-PPy	199	14	6620	[60]
6	PPy-ZrO <sub>2</sub>	1265	28	378	This work

Potential (scan rates), “m” is an active mass of the sample, and “ΔV” represents the potential window. The specific capacitance of PPy-10% ZrO<sub>2</sub> nanocomposite at various scan rates is calculated as given in Table 3. The specific capacitance (Cs) is reduced by increasing the scan rates, which makes the material resistive due to polarization [53]. Therefore, in PPy-ZrO<sub>2</sub> composite develops a simple track for the movement of ions that may raise the electrical conductivity which is very important to improve the specific capacitance. The CV curves of ZrO<sub>2</sub>, PPy, and PPy-ZrO<sub>2</sub> composite appear equivalent to an ideal rectangular shape through pseudo-capacitance properties [54]. The specific capacitance of ZrO<sub>2</sub>, PPy, and PPy-ZrO<sub>2</sub> composite at 10 mV/s scan rate is calculated as assumed in Table 2. In charge storage devices the necessary behavior of electrode material is confirmed through electrochemical impedance spectroscopy (EIS). The Nyquist plot for charge storage devices consists of vertical lines at high-frequency regions though, a half-circle performed at a low-frequency region can show the low electrical conductivity. A decrease in conductivity region suggests the interfacial charge transfer resistance [55]. Electrode materials’ conductance was analyzed using the equivalent series resistance (ESR) method.

#### 4.5. Electrochemical impedance spectroscopic analysis

The ESR of ZrO<sub>2</sub> is ~ 14 Ω, PPy is ~ 13 Ω, and PPy-ZrO<sub>2</sub> composite is obtained ~ 11 Ω. The ESR of PPy-ZrO<sub>2</sub> is low as compared to ZrO<sub>2</sub>, and PPy shows an increase in electrical conductivity due to the addition of ZrO<sub>2</sub> in PPy as exposed in Fig. 5(a). The PPy-ZrO<sub>2</sub> composite is nearly similar to the ideal capacitor and has well-straight lines as equated to others. The pure ZrO<sub>2</sub>, PPy, and PPy-ZrO<sub>2</sub> composite may have a semicircle at a high-frequency region which can improve the diffusion path length of ions and produce a hurdle to the motion of ions. The PPy-ZrO<sub>2</sub> composite may have a low impedance in its capacitance part and can show a better supercapacitor electrode material as equated to other electrode materials. Figure 5(b) shows the charge–discharge potential against

time-dependent curves for pure ZrO<sub>2</sub>, PPy, and PPy-10% ZrO<sub>2</sub> composite electrodes. The PPy and its composite give two disparities, slope, and perfect variations. The variation below near 0.5 V shows double-layer-capacitance performance from charge segregation at the electrode/electrolyte boundary. A slope variation nearly above 0.2 V specifies a characteristic pseudo-capacitance performance produced due to redox reaction at the electrode/ electrolyte boundary. Capacitance, energy density as well as power density of an electrode material can be calculated from the discharging curves using the following formulae:

$$C = I \times t / m \times \Delta V \quad (2)$$

$$E = 0.5 \times C_s \times (\Delta V)^2 / 3.6 \quad (3)$$

$$P = E \times 3600 / \Delta t \quad (4)$$

The PPy-10%ZrO<sub>2</sub> composite exhibits heightened capacitance, energy density, and power density compared to pure PPy and ZrO<sub>2</sub>. It can be observed that the capacitance of the nanocomposite is more than the sum of ZrO<sub>2</sub> and PPy (Table 4). Here, ZrO<sub>2</sub> gives a conductive path and presents a large surface area to support the material for PPy. Consequently, it improves the electrode to electrolyte zones and also allows the electrolyte ions to move fast through the electrode during the process of charge/discharge. The electrochemical characteristics are better efficient and are helpful for supercapacitor applications. Table 5 lists the electrochemical data for the PPy-10%ZrO<sub>2</sub> sample, providing a comparison with previously reported materials. The High performance of the designed electrode could be attributed to its specific structure and high conductivity, leading to the fast shuttling of ions and electrons at the electrode–electrolyte interface.

## 5. Conclusion

A composite of polypyrrole-doped zirconium dioxide was prepared by an in situ polymerization route. XRD results validated the presence of ZrO<sub>2</sub>-particles in PPy, which confirmed the successful formation of a composite. The

SEM image confirms the platelet structure in the PPy-ZrO<sub>2</sub> composite. This type of composition is excellent for charge storage device applications. The charging time is reduced, and the discharging time is enhanced, which can result in decreased internal resistance. Maximum capacitance of 1265 Fg<sup>-1</sup> at 1 Ag<sup>-1</sup> is seen for PPy-ZrO<sub>2</sub> electrodes. The energy density of 28 Wh kg<sup>-1</sup> is attained at 378 W kg<sup>-1</sup> (power density) with impedance decreased from pristine PPy ~ 13 Ω to PPy-10% ZrO<sub>2</sub> ~ 11 Ω composite. The synthesized composite material is an excellent semiconductor material for charge storage device applications as an electrode material consisting of ZrO<sub>2</sub> as a conducting improver.

**Acknowledgements** This research was funded by Researchers Supporting Project number (RSPD2024R762), King Saud University, Riyadh, Saudi Arabia.

**Author contributions** All authors made an equal contribution to this work. WA, FZ and MI conceived the idea. GFBS synthesized the material, while WA and BAA analyzed the data. WA, BAA and SMHQ formatted the initial draft, and the manuscript was collectively written by all authors. The final version of the manuscript has been approved by all authors.

**Data availability statement** All the related data is available from the authors upon request.

#### Declarations

**Conflict of interest** The authors declare that they have no known competing financial interests or personal relationships that could have appeared to influence the work reported in this paper.

**Author agreement statement** We, the undersigned, declare that this manuscript is original, has not been published before and is not currently being considered for publication elsewhere. We confirm that the manuscript has been read and approved by all named authors and that there are no other persons who satisfied the criteria for authorship but are not listed. We further confirm that all have approved the order of authors listed in the manuscript of us.

#### References

- [1] I D Parker *J. Appl. Phys.* **75** 1656 (1994)
- [2] N Akhtar, M Rani, S Ashraf, S Musaddiq, A Munawar and W Abbas *Modeling and Simulation of Functional Nanomaterials for Forensic Investigation* p 1 (2023)
- [3] H Jeon *Appl. Phys. Lett.* **60** 2045 (1992)
- [4] D Patnaik, S N Das and P P Nayak *Physics* **98** 2299 (2024)
- [5] S Kalingani, S N Das, S Bhuyan and L Sahoo *Trans. Electr. Electron. Mater.* **11** (2024)
- [6] S Kalingani, S N Das and S Bhuyan *Inorg. Chem. Commun.* **159** 111731 (2024)
- [7] A G Rolo, L G Vieira, M J M Gomes, J L Ribeiro, M S Belsley and M P Dos Santos *Thin Solid Films* **312** 348 (1998)
- [8] L Sahoo, S Bhuyan and S N Das *Appl. Phys. A* **128** 1136 (2022)
- [9] L Sahoo, S Bhuyan and S N Das *Condens. Matter.* **654** 414705 (2023)
- [10] Kalingani, S N Das and S K Pradhan *Trans. Electr. Electron. Mater.* **24** 31 (2023)
- [11] A Hirvonen, R Nowak, Y Yamamoto, T Sekino and K Niihara *J. Eur. Ceram. Soc.* **26** 1497 (2006)
- [12] D W Park and J C Ray *J. Ind. Eng. Chem.* **12** 142 (2006)
- [13] W Abbas, M E Mazhar, J Ahmad, S Ahmad, H M Khan, I Khan and M Ahmad *Physica Scripta* **97** 075004 (2022)
- [14] X A Zhang, Y Tang, F Zhang and C S Lee *Adv. Energy Mater.* **6** 1502588 (2016)
- [15] M Wang, C Jiang, S Zhang, X Song, Y Tang and H M Chen *Nat. Chem.* **10** 667 (2018)
- [16] A Heidari and C Brown *J. Nanomed. Res.* **2** 20 (2015)
- [17] R Ferro and J A Rodriguez *Solar Energy Mater. Solar Cells* **64** 363 (2000)
- [18] Y Liu, Y C Zhang and X F Xu *J. Hazard. Mater.* **163** 1310 (2009)
- [19] H Lu, L Liao, J Li, D Wang, H He, Q Fu and Y Tian *J. Phys. Chem. B* **110** 23211 (2006)
- [20] J yang, J Shang, Q Liu, X Yang, Y Tan, Y Zhao and Y Tang, *Angewandte Chemie.* e202406182 (2024)
- [21] X Bai, M Xu, Q Li and L Yu *Adv. Space Res.* **70** 825 (2022)
- [22] H Koezuka and A Tsumura *Synth. Metals* **28** 753 (1989)
- [23] G Gustafsson, G M Treacy, Y Cao, F Klavetter, N Colaneri and A J Heeger *Synth. Metals* **57** 4123 (1993)
- [24] J C Chiang and A G MacDiarmid *Synth. Metals* **13** 193 (1986)
- [25] R M Obodo, S M Mbam, H E Nsude, M Ramzan, S C Ezike, I Ahmad and F I Ezema *Appl. Surf. Sci. Adv.* **9** 100254 (2022)
- [26] R M Obodo, H E Nsude, S C Ezike, C Ononogbo, I Ahmad, M Maaza and F I Ezema *Hybrid Adv.* **5** 100143 (2024)
- [27] G Jiang *Appl. Sci. Manuf.* **33** 745 (2002)
- [28] M J Sailor, E J Ginsburg, C B Gorman, A Kumar, R H Grubbs and N S Lewis *Science* **249** 1149 (1990)
- [29] S C Ezike, A D Ahmed, R M Obodo and M A Salawu *Hybrid. Adv.* **1** 100006 (2022)
- [30] B Alkali, J B Yerima, A D Ahmed and S C Ezike *Optik* **270** 170072 (2022)
- [31] L Li, J Jiang and F Xu *Mater. Lett.* **61** 1091 (2007)
- [32] M M Ayad and E A Zaki *Eur. Polym. J.* **44** 3741 (2008)
- [33] S F Chung, T C Wen and A Gopalan *Mater. Sci. Eng.: B* **116** 125 (2005)
- [34] S C Ezike, C N Hyelnasinyi, M A Salawu, J F Wansah, A N Ossai and N N Agu *Surf. Interfaces* **22** 100882 (2021)
- [35] A N Ossai, S C Ezike, P Timtere and A D Ahmed *Chem. Phys. Impact.* **2** 100024 (2021)
- [36] A S Roy, K R Anilkumar and M A Prasad *J. Appl. Polym. Sci.* **123** 1928 (2012)
- [37] H P Wante, J Aidan and S C Ezike *Curr. Res. Green Sustain. Chem.* **4** 100218 (2021)
- [38] N A Niaz, A Shakoor, M Imran, N R Khalid, F Hussain, H Kanwal and S Afzal *J. Mater. Sci.: Mater. Electron.* **31** 11344 (2020)
- [39] M N ur Rehman, T Munawar, M S Nadeem, F Mukhtar, A Maqbool, M Riaz and F Iqbal *Ceram. Int.* **47** 18497 (2021)
- [40] N Boutaleb, F Z Dahou, H Djelad, L Sabantina, I Moulefera and A Benyoucef *Polymers.* **14** 4562 (2022)
- [41] M Zenasni, H Belhadj, M Kiari, M Alelyani, A B Alhailiy, A Benyoucef and Y Bakkour *Front. Energy Res.* **11** 1244699 (2023)
- [42] R Ullah, M Khan, R Khattak, N Khan, M S Khan and Y A El-Badry *Polymers.* **13** 4035 (2021)
- [43] C S Ferreira, SC Domenech and P. Lacaze, *J Appl Electrochem.* **31** 49 (2001)
- [44] B Garcia *J. Electrochem. Soc.* **149** 560 (2002)
- [45] H A Yoneyama, A Kishimoto and S Kuwabata *J. Chem. Soc. Chem. Commun.* **1** 986 (1991)

- [46] T K Vishnuvardhan, V R Kulkarni, C Basavaraja and S C Raghavendra *Bull. Mater. Sci.* **29** 77 (2006)
- [47] M Irfan, A Shakoor, A Majid, N Hassam and N Ahmed *Polym. Sci. Ser. A* **61** 105 (2019)
- [48] X Xu and X Wang *Nano Res.* **2** 891 (2009)
- [49] A Shakoor, T Z Rizvi, H U Farooq, N Hassan, A Majid, M Saeed and M Farooq *Polym. Sci. Ser. A* **55** 279 (2013)
- [50] W L Bragg *Scientia* **45** 153 (1929)
- [51] M A Chougule, S G Pawar, P R Godse, R N Mulik, S Sen and V B Patil *Soft Nanosci. Lett.* **1** 6 (2011)
- [52] C Yao and Y Tong *Trends Anal. Chem.* **39** 60 (2012)
- [53] W Abbas, Q Liu, N Akhtar, J Ahmad, M E Mazhar, T Li and J Gu *J. Electroanal. Chem.* **853** 113560 (2019)
- [54] C W Liew, S Ramesh and A K Arof *Energy* **109** 546 (2016)
- [55] A Varghese *Mater. Today Chem.* **29** 101424 (2023)
- [56] S Palsaniya, H B Nemade and A K Dasmahapatra *J. Phys. Chem. Solids* **154** 110081 (2021)
- [57] W K Chee, H N Lim, I Harrison, K F Chong, Z Zainal, C H Ng and N M Huang *Electrochimica Acta* **157** 88 (2015)
- [58] S Ishaq, M Moussa, F Kanwal, M Ehsan, M Saleem, T N Van and D Losic *Sci. Rep.* **9** 5974 (2019)
- [59] S Grover, S Shekhar, R K Sharma and G Singh *Electrochimica Acta* **116** 137 (2014)
- [60] Y J Peng, T H Wu, C T Hsu, S M Li, M G Chen and C C Hu *J. Power Sources* **272** 970 (2014)

**Publisher's Note** Springer Nature remains neutral with regard to jurisdictional claims in published maps and institutional affiliations.

Springer Nature or its licensor (e.g. a society or other partner) holds exclusive rights to this article under a publishing agreement with the author(s) or other rightsholder(s); author self-archiving of the accepted manuscript version of this article is solely governed by the terms of such publishing agreement and applicable law.